(11) Lee, T. J.; Schaefer, H. F., III. *J. Chem. Phys.* **1986**, *85*, 3437. Lindh, R.; Rice, J. E.; Lee, T. J. *J. Chem. Phys.* **1991**, *94*, 8008.
(12) Büchler, A.; Stauffer, J. L.; Klemperer, W.; Wharton, L. *J. Chem. Phys.* **1963**, *39*, 2299.
(13) (a) Gole, J. L.; Siu, A. K. Q.; Hayes, E. F. *J. Chem. Phys.* **1973**, *58*, 857. (b) Yarkony, D. R.; Hunt, W. J.; Schaefer, H. F., III. *Mol. Phys.* **1973**, *26*, 941. (c) Klimenko, N. M.; Musaev, D. G.; Charkin, O. P. *Russ. J. Inorg. Chem.* **1984**, *29*, 639. (d) v. Szentpály, L.; Schwerdtfeger, P. *Chem. Phys. Lett.* **1990**, *170*, 555. (e) Salzner, U.; Schleyer, P. v. R. *Chem. Phys. Lett.* **1990**, *172*, 461. (f) Hassett, D. M.; Marsden, C. J. *J. Chem. Soc., Chem. Commun.* **1990**, 667. (g) Dyke, J. M.; Wright, T. G. *Chem. Phys. Lett.* **1990**, *169*, 138. (h) DeKock, R. L.; Peterson, M. A.; Timmer, L. K.; Baerends, E. J.; Vernooijs, P. *Polyhedron* **1990**, *9*, 1919.
(14) Seijo, L.; Barandiaran, Z.; Huzinaga, S. *J. Chem. Phys.* **1991**, *94*, 3762.
(15) (a) Kaupp, M.; Schleyer, P. v. R.; Stoll, H.; Preuss, H. *J. Am. Chem. Soc.* **1991**, *113*, 6012. (b) Kaupp, M.; Schleyer, P. v. R. *J. Am. Chem. Soc.* **1992**, *114*, 491.
(16) DeKock, R. L.; Remington, R. B.; Schaefer, H. F., III. Unpublished manuscript, personal communication.
(17) Kutzelnigg, W. *Einführung in die Theoretische Chemie*, Vol. 2, *Die Chemische Bindung*; Verlag Chemie: Weinheim, Germany, 1978; p 486.
(18) Szasz, L. *Pseudopotential Theory of Atoms and Molecules*; Wiley: New York, 1985.
(19) Kaupp, M.; Schleyer, P. v. R.; Stoll, H.; Preuss, H. *J. Chem. Phys.* **1991**, *94*, 1360.
(20) Nicklass, A. Diplomarbeit, Universität Stuttgart, 1990.
(21) Dolg, M. Dissertation, Universität Stuttgart, 1989.
(22) Igel,-Mann, G.; Stoll, H.; Preuss, H. *Mol. Phys.* **1988**, *65*, 1321.
(23) Clark, T.; Chandrasekhar, J.; Spitznagel, G. W.; Schleyer, P. v. R. *J. Comput. Chem.* **1983**, *4*, 294.
(24) *Gaussian Basis Sets for Molecular Calculations*; Huzinaga, S., Ed.; Elsevier: New York, 1984.
(25) Poppe, J.; Igel-Mann, G.; Savin, A.; Stoll, H. Unpublished results. Kaupp, M.; Stoll, H.; Preuss, H. *J. Comput. Chem.* **1990**, *11*, 1029.
(26) Dunning, T. H.; Hay, P. J. In *Methods of Electronic Structure Theory*; Schaefer, H. F., III, Ed.; Modern Theoretical Chemistry, Vol. 3; Plenum Press: New York, 1977; p 1.
(27) Møller, C.; Plesset, M. S. *Phys. Rev.* **1934**, *46*, 618.
(28) (a) Meyer, W. *J. Chem. Phys.* **1973**, *58*, 1017. (b) Meyer, W. *Theor. Chim. Acta* **1974**, *35*, 227. (c) Meyer, W. *J. Chem. Phys.* **1976**, *64*, 2901.
(29) Frisch, M. J.; Head-Gordon, M.; Schlegel, H. B.; Raghavachari, K.; Binkley, J. S.; Gonzalez, C.; DeFrees, D. J.; Fox, D. J.; Whiteside, R. A.; Seeger, R.; Melius, C. F.; Baker, J.; Kahn, L. R.; Stewart, J. J. P.; Fluder, E. M.; Topiol, S.; Pople, J. A. *Gaussian 88*; Gaussian, Inc.: Pittsburgh, PA, 1988.
(30) Werner, H. J.; Knowles, P. J. Program MOLPRO, 1987, see, e.g.: (a) Werner, H. J. *Adv. Chem. Phys.* **1987**, *69*, 1. (b) Werner, H. J.; Knowles, P. J. *J. Chem. Phys.* **1988**, *89*, 5803. (c) Knowles, P. J.; Werner, H. J. *Chem. Phys. Lett.* **1988**, *145*, 514.
(31) Kaupp, M.; Schleyer, P. v. R.; Dolg, M.; Stoll, H. *J. Am. Chem. Soc.* **1992**, *114*, 8202.
(32) Frenking, G.; Koch, W.; Collins, J. P. *J. Chem. Soc., Chem. Commun.* **1988**, 1147. Koch, W.; Frenking, G.; Gauss, J.; Cremer, D. *J. Am. Chem. Soc.* **1986**, *108*, 5808.
(33) Green, S. *J. Chem. Phys.* **1971**, *54*, 827. Grimaldi, F.; Lecourt, A.; Moser, C. *Int. J. Quantum Chem., Symp.* **1967**, *1*, 153.
(34) (a) Boys, S. F.; Bernardi, F. *Mol. Phys.* **1970**, *19*, 553. (b) Recent studies indicate that the counterpoise correction does not generally give an upper bound to the true BSSE and is not necessarily a good estimate: Schwenke, D. W.; Truhlar, D. G. *J. Chem. Phys.* **1985**, *82*, 2418. Frisch, M. J.; DelBene, J. E.; Binkley, J. S.; Schaefer, H. F., III. *J. Chem. Phys.* **1986**, *84*, 2279.
(35) Jacox, M. E. *J. Mol. Spectrosc.* **1985**, *113*, 286.
(36) Utamapanya, S.; Ortiz, J. V.; Klabunde, K. J. *J. Am. Chem. Soc.* **1989**, *111*, 799.

Diffusion Effects on Pyrene Excimer Kinetics: Determination of the Excimer Formation Rate Coefficient Time Dependence[1]

J. Duhamel, M. A. Winnik,*

Lash Miller Chemical Laboratories, Department of Chemistry and Erindale College, University of Toronto, Toronto, Ontario M5S 1A1, Canada

F. Baros, J. C. André,

ENSIC-INPL, BP 451 F54001 Nancy Cedex, France

and J. M. G. Martinho

Centro de Química-Física Molecular, Instituto Superior Técnico, 1096 Lisboa Codex, Portugal
(Received: April 8, 1992; In Final Form: August 11, 1992)

A numerical method is presented to recover the excimer formation rate coefficient from the experimental monomer and excimer decay curves. This method was applied to study pyrene monomer–excimer kinetics in cyclohexanol from 25 °C up to 85 °C. We observed that the time evolution of the rate coefficient deviates from the Smoluchowski equation, showing a minimum at high temperatures and concentrations, when the reversibility effects are more pronounced.

I. Introduction

Since the earliest days of this century there has been special interest in the rate of reactions that are influenced by the diffusive motion of the reactants. Many types of processes fall within this category: aggregation phenomena, enzyme–substrate binding, reassociation of photodissociated pairs, relaxation phenomena following pH or temperature jump, and fluorescence and phosphorescence quenching reactions. The feature that distinguishes these processes is the early time behavior, in which the redistribution of the reactants competes with the intrinsic chemical reaction step.

With the recent developments in picosecond lasers and improved fluorescence quenching measurements, it is now possible to study these transient effects with greater precision. The forward reaction rate for diffusion-influenced processes[2-5] is normally described in terms of a time-dependent rate coefficient $k_f(t)$. For irreversible reactions, $k_f(t)$ decays from its initial value at $t = 0$ to a steady-state value k_f^s. At times not too close to zero, the decay takes the form

$$k_f(t) = 4\pi N'_A D\sigma'_{eff}\left[1 + \frac{\sigma'_{eff}}{(\pi Dt)^{1/2}}\right] \quad (1)$$

where N'_A is Avogadro's number per millimole, σ'_{eff} is an effective reaction radius, and D is the mutual diffusion coefficient of the reactants. In recent years, good experimental evidence has been provided in support of this behavior from fluorescence quenching measurements.[6-9]

For reversible reactions, the description of the reaction kinetics is much more complex.[10-14] Conceptually, one imagines that the reverse reaction generates reactants at different times in close

* To whom correspondence should be addressed.

0022-3654/92/2096-9805$03.00/0

proximity. These can react faster than the uncorrelated pairs distributed in the bulk solution. As a consequence, $k_f(t)$ for reversible reactions might be expected to decay, pass through a minimum, and subsequently increase in magnitude, owing to the successive creation of reactive species.

Here we present the first experimental evidence that this idea is correct. We examine the kinetics of pyrene excimer formation at high concentration in a viscous solvent and analyze the data by a novel method. This technique, the "β-method" proposed recently by Duhamel et al.,[15] allows one to calculate values for $k_f(t)$ point by point. Thus it avoids the need, for data analysis, to develop a theoretical formulation for the time dependence of $k_f(t)$ for reversible reactions.

We begin with a short review of the kinetics of reactions operating under the influence of diffusion, followed by a discussion of excimer kinetics and the β-method for data analysis. We then present and analyze picosecond fluorescence decay data for pyrene in cyclohexanol over a series of temperatures to show, indeed, that under some circumstances $k_f(t)$ passes through a minimum and increases to a steady-state value.

II. Experimental Part

The fluorescence decay curves were obtained by the single-photon counting technique. The excitation source is composed of a mode-locked Nd:YAG laser (Coherent Model 76-s) whose output frequency is doubled by a KTP crystal giving pulses of 70-ps full width at half-maximum (FWHM) at 532 nm for a 76-MHz repetition rate. This output beam is used to synchronously pump Rhodamine 6G in a cavity-dumped dye laser (Coherent Model 701-3). At a repetition rate of 380 kHz, pulses of about 10-ps FWHM are obtained at 620 nm. This frequency is then doubled with a KTP crystal in order to get a UV pulse at 310 nm. The residual fundamental beam is directed to a Hamamatsu S2840 high-speed PIN silicon photodiode that triggers the stop signal (inverse mode) of the time to amplitude converter (TAC). The fluorescence signal, collected either front-face or at right angles (depending on the concentration of the sample), is selected by a grating monochromator (PTI 1200 grooves/mm, blazed at 500 nm) and viewed by a Hamamatsu R1564U-01 MCP photodetector, whose output after being amplified is used as the start signal of the TAC. The output signals of the TAC are stored in a multichannel analyzer plug in board in a PC-386-type personal computer.

Fluorescence spectra were recorded on a Spex Fluorolog 2 spectrofluorimeter.

Pyrene was zone refined (100 steps) and the cyclohexanol (spectrograde, Kodak) was used as received. The purity of the solvent was checked by UV–vis absorption and fluorescence and no impurity traces were detected. A dilute solution ([Py] = 2.0×10^{-6} M) and two concentrated ones ([Py] = 1.0×10^{-2} and 8.9×10^{-2} M) were prepared and degassed by freeze–pump–thaw involving as many cycles as necessary (typically 7) until no bubbles were seen during a thaw step. The experiments were temperature controlled by a temperature bath, with an estimated temperature precision of ±0.5 °C. The pyrene monomer fluorescence decay curves were observed at 376 nm and the excimer decays at 520 nm with at least 20000 counts in the most populated channel over 1024 channels. When analyzing fluorescence decays by a mono-, bi-, and triexponential fitting, the δ function convolution method (DFCM)[16] was used. When the fluorescence decay curves are fitted with a decay function that includes a transient term, a mimic instrumental response function is recovered from the decay of a reference compound. Decay curves of diluted degassed solutions of 2,5-diphenyloxazole (PPO) in cyclohexane (τ = 1.37 ns) and the decay of 2,5-bis(5-*tert*-butyl-2-benzoxazolyl)thiophene (BBOT) in ethanol (τ = 1.47 ns) were used for the fit of monomer and excimer decay curves, respectively.

III. Brief Review

There is a vast literature on the theory of diffusion-influenced reactions. Fortunately there are a number of very useful reviews.[2-5] The time dependence of $k_f(t)$ for diffusion-influenced reactions comes about in the following way: consider a reaction initiated at time $t = 0$, as with a δ-pulse of light, to produce the reactant A*, which reacts with B. When molecular diffusion is slower than the reaction step, surviving A* at times greater than zero experience a depletion in the local concentration of B. The local concentration can be written as the product of the bulk concentration [B] times the density distribution function, $\rho(r,t)$, the rate equation being given by

$$d[A^*]/dt = -k_{eq}\rho(\sigma',t)[B][A^*] \quad (2)$$

where k_{eq} is the bimolecular rate constant that would describe the reaction if the equilibrium distribution of B around A* could be maintained at all times and $\rho(\sigma',t)$ is the density distribution function at the reacting distance, σ'. We normally define the reaction rate coefficient in terms of the bulk concentration of reactants. As a consequence, we define $k_f(t)$ in terms of the expression

$$d[A^*]/dt = -k_f(t)[B][A^*] \quad (3)$$

Thus $k_{eq} = k_f(0)$, and the time dependence of $k_f(t)$ is simply a convenient way of representing the influence of the time evolution of $\rho(\sigma',t)$ on the reaction rate.

A bimolecular reaction in solution can be thought of in terms of consecutive diffusion and reaction steps, as in Scheme I, where

SCHEME I

$$A^* + B \underset{k_{-D}}{\overset{k_D}{\rightleftharpoons}} A^*\cdots B \underset{k_{-R}}{\overset{k_R}{\rightleftharpoons}} E^*$$

A* and B are reactants, (A*···B) is the encounter complex, E* represents the products, k_D and k_{-D} are the rate constants for the formation and dissociation of the encounter complex, and k_R and k_{-R} are the rate constants for the forward and reverse reactions.

Under the typical conditions considered by Noyes[3] (large volume, dilute solutions, [B] ≫ [A*], and only hard-sphere interactions between reactants), and if the k_{-R} step can be neglected, the forward rate coefficient is described by the expression

$$k_f(t) = k_f^s[1 + a \exp(b^2 t) \operatorname{erfc}(bt^{1/2})] \quad (4)$$

Here $a = k_{eq}/k_D$, $b = D^{1/2}(k_{eq} + k_D)/(\sigma' k_D)$, and D is the mutual diffusion coefficient of the reactants. The value of $k_f(t)$ is initially large ($k_f(0) = k_{eq}$) and decays at long times to a steady-state value, k_f^s, which in turn is related to k_{eq}

$$k_f^s = \frac{k_{eq}k_D}{k_{eq} + k_D} \quad (5)$$

Equation 4 can be considerably simplified by expanding the complementary error function (erfc (x)) in a power series and keeping only the first term. In this way one obtains eq 1, with σ'_{eff} related to the reaction radius, σ', by

$$\sigma'_{eff} = \frac{k_{eq}}{k_{eq} + k_D}\sigma' \quad (6)$$

with

$$k_D = 4\pi N'_A D\sigma' \quad (7)$$

Note that we distinguish the reaction radius, σ', from the collision radius, σ, since one commonly expects $\sigma' > \sigma$.

Equation 1 contains three features of interest. The first is the well-known $t^{-1/2}$ dependence of the transient part of $k_f(t)$, first elaborated by Smoluchowski.[17] The second is that the effect of a finite k_R is to renormalize σ' for a strictly diffusion-controlled reaction to $\sigma'_{eff} < \sigma'$. The third point, of particular interest here, is that for irreversible reactions $k_f(t)$ decays monotonically to its steady-state value, $k_f^s = 4\pi N'_A D\sigma'_{eff}$.

IV. Excimer Kinetics and the β-Method

The mechanism of excimer formation and decay is presented in Scheme II.[17] The locally excited monomer A*, produced by a pulse of light I, may decay with intrinsic rate constant k_A or form the excimer, E*, with rate coefficient $k_1(t)$, on the encounter

SCHEME II

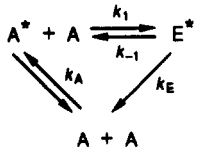

of the excited species A* with a ground state monomer A. Once formed, the excimer can dissociate with rate constant k_{-1} to reform the excited-plus-unexcited monomers or decay to two ground-state monomers with the intrinsic rate constant k_E.

The monomer–excimer kinetics is described by the rate equations

$$d[A^*]/dt = I + k_{-1}[E^*] - (k_A + k_1(t)[A])[A^*] \quad (8)$$

$$d[E^*]/dt = k_1(t)[A][A^*] - (k_E + k_{-1})[E^*] \quad (9)$$

If A* is created by absorption of a δ-pulse of light and k_1 is time independent, the concentration of A* and E* follows the well-known biexponential decay law[18]

$$[A^*(t)] = \frac{[A^*(0)]}{\lambda_2 - \lambda_1}\{(\lambda_2 - X)\exp(-\lambda_1 t) + (X - \lambda_1)\exp(-\lambda_2 t)\} \quad (10)$$

$$[E^*(t)] = \frac{k_1[A][A^*(0)]}{\lambda_2 - \lambda_1}\{\exp(-\lambda_1 t) - \exp(-\lambda_2 t)\} \quad (11)$$

with

$$2\lambda_{1,2} = \{(X + Y) \mp [(X - Y)^2 + 4k_{-1}k_1[A]]^{1/2}\} \quad (12)$$

and

$$X = k_A + k_1[A]; \qquad Y = k_E + k_{-1} \quad (13)$$

The time-independence of k_1 would be maintained in a natural way if $k_1 \ll k_D$ and the excimer formation step were a purely chemical process. Excimer formation, however, is commonly considered to be diffusion influenced and so k_1 must be time-dependent. Nevertheless, the integration of eq 9 gives

$$[E^*] = k_1(t)[A^*][A] \otimes \exp\{-(k_E + k_{-1})t\} \quad (14)$$

where $\otimes$ denotes convolution. This equation was first used by Martinho,[19] to analyze simultaneously the monomer and excimer decay curves of pyrene solutions under conditions where the back reaction is very slow and $k_1(t) \cong k_f(t)$ (see eq 1). From the simultaneous fit of monomer and excimer decays the transient term of $k_f(t)$ was obtained, allowing the evaluation of the mutual diffusion coefficient and the effective reaction radius, when the stationary part of $k_f(t)$ is known. When the back reaction is significant (high temperatures, excimer-forming fluorophores with high k_{-1} rate constant), eq 14 cannot be used to analyze the experimental decay curves, since $k_1(t)$ is unknown. When reversibility is significant, $k_1(t)$ deviates strongly from $k_f(t)$, becoming a complex function of time, depending on k_{-1}, the fluorophore concentration, and the intrinsic lifetimes of the monomer and the excimer.[10] The evaluation of the correct excimer formation rate equation is a very subtle question that can be solved by the correct formulation of the time evolutions of the monomer and excimer concentrations followed by coupling of these expressions with the kinetic rate equations. We believe that the validity of the rate equations is now well established,[10a,13,14b] although its validity has been questioned in the past.[20] This misunderstanding results from the incorrect use of $k_f(t)$ instead of $k_1(t)$ in the kinetic rate equations when the back reaction is important.

What is an appropriate strategy for obtaining the rate coefficients for excimer kinetics? We believe that the most effective approach recognizes that, under most circumstances, the contribution of the transient effect to the reaction kinetics is small and that analysis of the individual monomer and excimer decay profiles in terms of Scheme I and time-independent rate coefficients provides meaningful values of k_E, k_{-1}, and k_1, the long-time, steady-state value of $k_1(t)$. Values obtained over a range of temperatures and/or concentrations can then be extrapolated to a nearby temperature and concentration ranges where transient effects or the contribution of transient effects plus excimer reversibility makes a significant contribution to the data. Alternatively, if the decay curves are available at sufficiently short times where reversibility is negligible and $k_1(t)$ is given by eq 4, one can analyze the decay profiles to obtain the transient term and the steady-state value of $k_f(t)$. One can then use Arrhenius plots to extrapolate values of k_1, k_{-1}, and k_E to temperature ranges where the contribution of transient effects plus excimer dissociation is most troublesome to analyze. This is the strategy underlying the β-method for the point-by-point calculation of $k_1(t)$ from experimental data.

In traditional monomer–excimer studies, the monomer $[I_A(t)]$ and the excimer $[I_E(t)]$ decay curves are measured separately and analyzed independently. Here we point out that additional information about the system is available if the relative intensities of monomer and excimer fluorescence are also considered. In the β-method, this problem is dealt with by the introduction of a parameter β that normalizes the experimental excimer intensities. If $[A^*(t)] = I_A(t)$ and $[E^*(t)]$ is taken as being proportional to $I_E(t)$, one can write $[E^*(t)] = \beta I_E(t)$, where β is just a normalization factor. Thus we rewrite the rate equations (8) and (9), with the Dirac function $\delta(t)$, describing instantaneous sample excitation

$$\frac{dI_A(t)}{dt} = \delta(t) + k_{-1}\beta I_E(t) - (k_A + k_1(t)[A])I_A(t) \quad (15)$$

$$\beta\frac{dI_E(t)}{dt} = k_1(t)[A]I_A(t) - (k_E + k_{-1})\beta I_E(t) \quad (16)$$

and

$$\beta = -\frac{(dI_A(t)/dt) + k_A I_A(t)}{(dI_E(t)/dt) + k_E I_E(t)} \qquad t > 0 \quad (17)$$

for $k_1(t)$ one derives

$$k_1(t) = \frac{\beta}{[A]}\frac{(dI_E(t)/dt) + (k_E + k_{-1})I_E(t)}{I_A(t)} \qquad t > 0 \quad (18)$$

If k_E and k_{-1} can be determined independently, one can use these values in conjunction with the experimental decay profiles to calculate numerically $k_1(t)$ from eq 18.

V. Data and Data Analysis

The intrinsic lifetime of pyrene was obtained from the single-exponential decay curves of a 2×10^{-6} M solution of pyrene in cyclohexanol over the temperature range 25–85 °C. The Arrhenius plot of the reciprocal lifetime, $k_M = 1/\tau_M$, plotted in Figure 1, is linear with a very small activation energy of $\cong$0.8 kcal mol^{-1}.

We first fit our decay profiles to traditional models of fluorescence quenching to assess their sensitivity to factors associated with transient effects and excimer dissociation. Assuming that the excimer is irreversible and that $k_1(t)$ is given by the Smoluchowski equation (eq 1), one fits the monomer decay curve to the form

$$I_M(t) = A\exp(-ct - 2dt^{1/2}) \quad (19)$$

where

$$c = k_A + 4\pi N'_A D\sigma'_{eff}[A] \quad (20)$$

$$d = 4N'_A\sigma'_{eff}(\pi D)^{1/2}[A] \quad (21)$$

For the 1.0×10^{-2} M pyrene solution, this fit gives reasonable χ^2 over the entire range of temperatures, although the data obtained at $t > 45$ °C show poor fits as reflected in the autocorrelation of the residuals. For the highest concentration (8.9×10^{-2} M) a reasonable fit was obtained only at 25 °C. The values of D and σ'_{eff} are summarized in Table I. We note with interest that D values calculated from these data increase as they should with increasing temperature but appear to level off for data obtained at $t > 45$ °C. Values of σ'_{eff} show significant scatter but for the 1.0×10^{-2} M pyrene solution fall in the range 6–8 Å in the lower temperature range.

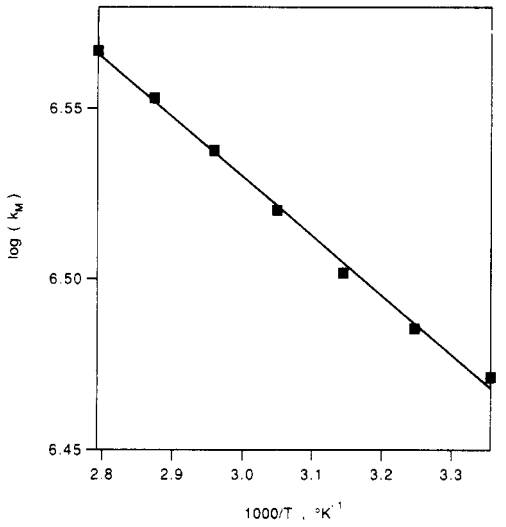

Figure 1. Arrhenius plot of the monomer decay rate constant, k_A in s^{-1}, for pyrene in cyclohexanol at 2×10^{-6} M.

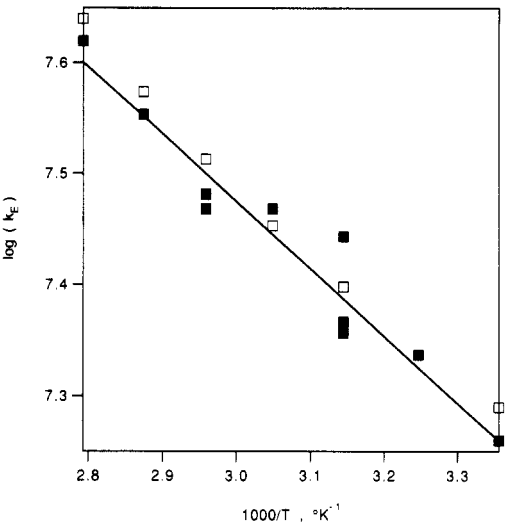

Figure 2. Arrhenius plot of the excimer decay rate constant, k_E in s^{-1}, obtained by the β-method for pyrene in cyclohexanol at two different pyrene concentrations (□, [Py] = 0.089 M; ■, [Py] = 0.01 M).

TABLE I: Results Obtained from the Analysis of the Monomer Fluorescence Decays of Pyrene in Cyclohexanol at Different Temperatures Using Eq 19

T/°C	$D/10^{-7}$ cm^2 s^{-1}	σ'_{eff}/Å	χ^2	[Py], M
25	4.0	8.2	1.3	0.010
	3.9	8.0	1.5	0.089
35	7.6	6.3	1.4	0.010
45	11.4	8.1	1.4	0.010
55	11.7	9.8	1.3	0.010
65	10.9	11.9	1.3	0.010
75	11.1	13.4	1.4	0.010
85	13.2	11.5	1.6	0.010

Classical Birks analysis predicts the same decay constants λ_1 and λ_2, from both monomer and excimer decay curves (eqs 10 and 11). For the monomer fit the ratio of the preexponential factors of the short and long lifetimes depends on the concentration and medium viscosity and can be very small. In order to achieve a better accuracy in the recovered lifetimes, a constrained fit of the monomer decay curves was performed, fixing the short or the long lifetimes to the values obtained in the excimer fit. The short lifetime was fixed for the concentrated solution ([Py] = 0.089 M) and the long one for the more dilute solution ([Py] = 0.01 M), because the corresponding preexponential factors are the lowest. Table II shows the ratios of the preexponential factors A_2/A_1 and lifetimes, τ_i (i = 1, 2), obtained from the fit of the monomer and excimer decay curves. Although the recovered free lifetime from the monomer fit matches the corresponding one from the excimer fit, this does not mean that Birks kinetics are obeyed. Indeed, large deviations from Birks kinetics predictions were detected at lower temperatures and high concentrations where the contribution of the transient effect plus reversibility would be most prominent. As we have pointed out previously,[19,21] one of the hallmarks of this effect is a systematic deviation of the ratio of preexponential factors in the excimer profile, A_2/A_1, to values significantly smaller than unity. As shown in Table II, A_2/A_1 values in the range of −0.85 are common to all the fits to the data for 8.9×10^{-2} M pyrene solution, accompanied by poor χ^2 values. Much higher A_2/A_1 values (ca. −0.95) and better values of χ^2 are found for the 1.0×10^{-2} M pyrene solution at temperatures above 55 °C. Here the contribution of the transient effects is small, while that of the excimer dissociation is larger. Table III shows the values of k_1, k_{-1}, and τ_E, calculated with eqs 10–13, from the data in Table II.

In order to obtain the time evolution of $k_1(t)$ from eq 18, it is necessary to know the values of τ_E and k_{-1}. The excimer lifetime was obtained by checking the stability of the β coefficient over the whole time domain of the experiment. Through trial estimates, one optimizes a value for $\tau_E = 1/k_E$ by calculating a pseudo-χ^2 equal to the sum of the residuals between the value of the β coefficient at a given time and the average value of the β coefficient over time

$$\langle\beta\rangle = \frac{1}{t_1 - t_2}\int_{t_1}^{t_1}\beta(t)\,dt \tag{22}$$

$$\chi^2 = \sum_{t=t_1}^{t_2}\left(1 - \frac{\beta(t)}{\langle\beta\rangle}\right)^2 \tag{23}$$

The excimer lifetime τ_E is kept when the χ^2 value is minimum. In this way the β coefficient and τ_E are obtained simultaneously. In order to perform the procedure described above, the monomer and excimer decay curves were arbitrarily fitted to sums of three exponential terms, and from this fit values of $I_A(t)$, $I_E(t)$, $dI_A(t)/dt$, and $dI_E(t)/dt$ were calculated. Figure 2 shows the Arrhenius plot

TABLE II: Parameters Obtained through a Two-Exponential Fitting (Eqs 10 and 11) of the Fluorescence Decays of the Monomer and the Excimer (in Parentheses) of Pyrene Solutions in Cyclohexanol at Different Temperatures for Two Concentrations

T/°C	τ_1/ns	τ_2/ns	A_2/A_1	χ^2	[Py]/M
25	176.3 (174.7)	37.9 (37.9)	0.078 (−0.84)	1.3 (1.5)	0.010
	54.1 (54.1)	29.4 (26.5)	12.8 (−0.86)	3.1 (2.3)	0.089
35	130.3 (128.4)	37.2 (37.2)	0.092 (−0.88)	1.2 (1.4)	0.010
	46.4 (46.4)	17.5 (15.6)	25.1 (−0.84)	3.4 (2.7)	0.089
45	95.5 (95.9)	32.4 (32.4)	0.104 (−0.94)	1.2 (1.4)	0.010
	40.9 (40.9)	11.3 (10.5)	23.8 (−0.84)	3.4 (1.9)	0.089
55	77.6 (76.2)	27.1 (27.1)	0.17 (−0.95)	1.2 (1.7)	0.010
	36.4 (36.4)	7.8 (7.4)	17.2 (−0.83)	2.3 (1.8)	0.089
65	68.2 (66.4)	21.7 (21.7)	0.24 (−0.95)	1.3 (1.3)	0.010
	32.4 (32.4)	5.7 (5.5)	11.2 (−0.83)	1.6 (1.4)	0.089
75	59.5 (59.5)	15.2 (15.2)	0.30 (−0.95)	1.2 (1.3)	0.010
	28.9 (28.9)	4.1 (3.9)	7.2 (−0.83)	1.7 (1.5)	0.089
85	59.4 (59.5)	10.6 (10.6)	0.29 (−0.94)	1.1 (1.4)	0.010
	26.1 (26.1)	3.1 (3.2)	4.8 (−0.93)	1.3 (1.6)	0.089

TABLE III: Results Obtained from the Values of Table II by Using Eqs 10–13

T/°C	k_1/M^{-1} ns^{-1}	k_{-1}/ns^{-1}	τ_E/ns	[Py]/M
25	0.42	0.068	55	0.010
	0.34	0.00054	52	0.089
35	0.62	0.0046	48	0.010
	0.59	0.00089	45	0.089
45	0.92	0.0039	40	0.010
	0.93	0.0019	40	0.089
55	1.3	0.0055	36	0.010
	1.3	0.0044	35	0.089
65	1.7	0.0089	32	0.010
	1.8	0.0099	30	0.089
75	2.5	0.017	27	0.010
	2.4	0.021	26	0.089
85	3.0	0.034	23	0.010
	3.0	0.043	22	0.089

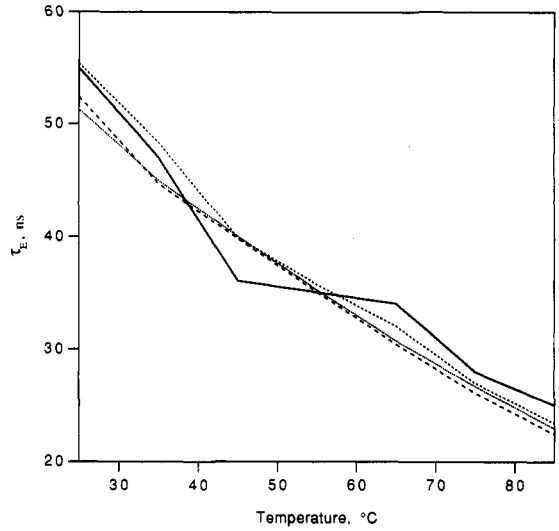

Figure 3. Comparison of the excimer lifetime τ_E for pyrene excimer in cyclohexanol obtained by fitting the data to the Birks model (---) τ_E (Birks method, [Py] = 0.01 M) and (– – –) τ_E (Birks method, [Py] = 0.089 M) and by using the β-method (—) τ_E (β-method, [Py] = 0.01 M) and (···) τ_E (β-method, [Py] = 0.089 M).

of $k_E = 1/\tau_E$ values obtained at each temperature. These τ_E values are compared in Figure 3 with the corresponding values obtained by the Birks' analysis (see Table III). The values of τ_E achieved by both methods are surprisingly very close in magnitude, which gives us some confidence in the results.

The one remaining unknown parameter is the excimer dissociation rate constant k_{-1}. We approach this problem by assuming that for the 1.0×10^{-2} M pyrene solution in the higher temperature range of accessible temperatures ($T \geq 55$ °C) the magnitude of the transient effects is relatively small and Birks' analysis gives reasonable results. Figure 4 shows the Arrhenius plot of k_{-1}. The experimental points fit to a straight line, from which k_{-1} values at lower temperatures were obtained.

The excimer formation rate coefficient can then be obtained from eq 18 for both concentrations in the full temperature range. Figure 5 shows the variation of $k_1(t)$ versus t for the 1.0×10^{-2} M solution. The time evolution of the rate coefficient for low temperatures agrees with the Smoluchowski expression but deviates at higher temperatures where a minimum begins to appear. The rate coefficient increases with temperature owing to the increase of the mutual diffusion coefficient. The $k_1(t)$ values for the 8.9×10^{-2} M pyrene solution are plotted in Figure 6. Here, the effect of reversibility is visible for low temperatures ($t > 45$ °C) with the appearance of a well-defined minimum for temperatures between 45 and 65 °C. The "steady-state" value attained at long times is higher than the stationary value of the Smoluchowski (Collins–Kimball) rate coefficient. At higher temperatures the contribution of transient effects to the rate coefficient decreases and the minimum disappears. This kind of behavior agrees qualitatively with the theoretical developments by Ber-

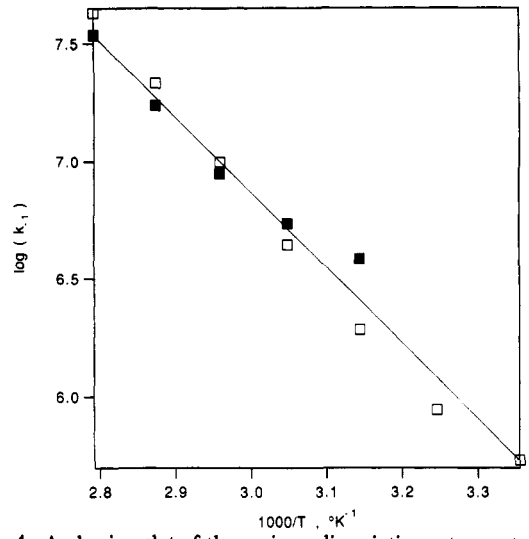

Figure 4. Arrhenius plot of the excimer dissociation rate constant, k_{-1} in s^{-1}, for pyrene in cyclohexanol at two different pyrene concentrations: (□, [Py] = 0.089 M; ■, [Py] = 0.01 M). The k_{-1} values have been obtained assuming a Birks kinetics model. Note that the assumptions in this model break down for [Py] = 0.01 M at $T < 50$ °C.

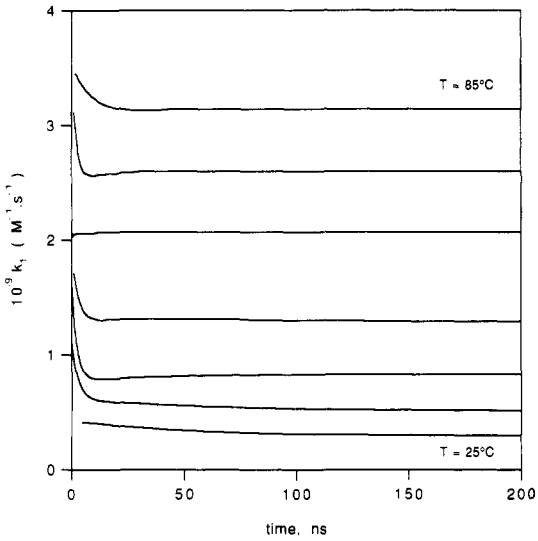

Figure 5. Apparent excimer formation rate coefficient for a solution of pyrene (0.01 M in cyclohexanol) at different temperatures shown in 10-deg intervals from 25 to 85 °C.

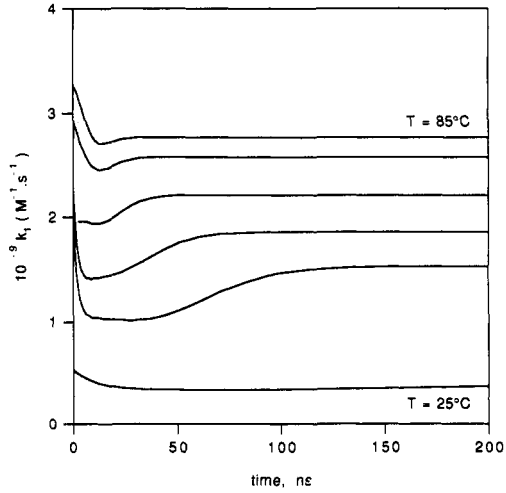

Figure 6. Apparent excimer formation rate coefficient for a solution of pyrene (0.089 M in cyclohexanol) at different temperatures (25, 45, 55, 65, 75, and 85 °C). The noise in the plot is that due to the point-by-point calculation of k_1, and we have chosen not to smooth the values in presenting the data.

beran-Santos and Martinho,[10] and Andrê, Baros, and Winnik.[12]

VI. Summary

By normalizing the excimer emission profile with respect to the monomer emission profile, the β-method provides a novel and an unambiguous method for determining k_E, the reciprocal decay time of the pyrene excimer. With this value and those of k_{-1} and β, one can compute values of $k_1(t)$, point by point, to assess its time evolution. In this analysis, values of k_{-1} are determined over a range of temperatures where the transient effects are small and then extrapolated via an Arrhenius expression to nearby temperatures where these effects are significant.

We make two very important observations about the time profile of $k_1(t)$ under conditions (high temperatures and pyrene concentrations) where excimer dissociation followed by excimer reformation is expected to be important. We see first that $k_1(t)$ decreases, passes through a minimum, and then increases to a steady-state value. We attribute this increase to excimer reformation from dissociated pairs. The second important consideration is that the steady-state value of k_1 found under these conditions is larger than that predicted for the case of irreversible processes and indicates that the local steady-state concentration is intermediate between that of irreversible processes and the initial bulk concentration of reactants.

Acknowledgment. J.D. and M.A.W. thank NSERC (Canada) for its support of this research. J.M.G.M. also thanks JNICT (Portugal) for financial support and INVOTAN for a fellowship.

Registry No. Pyrene, 129-00-0.

References and Notes

(1) This paper no. 11 in a series on transient effects on diffusion-controlled reactions by Toronto group and no. 25 in a similar series by the group in Nancy.
(2) Rice, S. A. In *Comprehensive Chemical Kinetics*; Bamford, C. H., Tipper, C. F. H., Compton, R. G., Eds.; Elsevier: New York; Vol. 25, 1985.
(3) Noyes, R. M. *Prog. React. Kinet.* **1961**, *1*, 129-60.
(4) Birks, J. B. In *Organic Molecular Photophysics*; Birks, J. B., Ed.; Wiley: New York, 1973; Chapter 8.
(5) Gösele, U. M. *Prog. React. Kinet.* **1984**, *13*, 63-161.
(6) Nemzek, T. L.; Ware, W. R. *J. Chem. Phys.* **1975**, *62*, 477-89.
(7) Lakowicz, J. R.; Johnson, M. L.; Gryczynski, I.; Joshi, N.; Laczko, G. *J. Phys. Chem.* **1987**, *91*, 3277.
(8) Joshi, G. C.; Bhatnagar, R.; Doraiswamy, S.; Periasamy, N. *J. Phys. Chem.* **1990**, *94*, 2908-14.
(9) Periasamy, N.; Doraiswamy, S.; Venkataraman, B.; Fleming, G. R. *J. Chem. Phys.* **1988**, *89*, 4799-806.
(10) (a) Berberan-Santos, M. N.; Martinho, J. M. G. *J. Chem. Phys.* **1991**, *95*, 1817-24. (b) Berberan-Santos, M. N.; Martinho, J. M. G. *Chem. Phys. Lett.* **1991**, *178*, 1-8. (c) Berberan-Santos, M. N.; Pinheiro, J. P.; Farinha, J. P.; Martinho, J. M. G. *J. Lumin.* **1991**, *48 & 49*, 456-58.
(11) Lee, S.; Karplus, M. *J. Chem. Phys.* **1987**, *86*, 2766-72.
(12) Andrê, J. C.; Baros, F.; Winnik, M. A. *J. Phys. Chem.* **1990**, *94*, 2942-48.
(13) (a) Szabo, A. *J. Chem. Phys.* **1991**, *95*, 2481-90. (b) Agmon, N.; Szabo, A. *J. Chem. Phys.* **1990**, *92*, 5270-84.
(14) (a) Sienicki, K.; Winnik, M. A. *J. Chem. Phys.* **1987**, *87*, 2766-72. (b) Sienicki, K.; Durocher, G. *J. Chem. Phys.* **1991**, *94*, 6590-97.
(15) (a) Duhamel, J. Thèse du doctorat, Université de Nancy, Nancy, France, 1990. (b) Duhamel, J.; Bouchy, M.; Baros, F.; Andrê, J. C. *J. Lumin.*, in press.
(16) Zuker, M.; Szabo, G.; Bramall, L.; Krajcarski, D. T.; Selinger, B. *Rev. Sci. Instrum.* **1985**, *56*, 14-22.
(17) Smoluchowski, M. *Z. Phys. Chem.* **1917**, *92*, 129-62.
(18) Birks, J. B. *Photophysics of Aromatic Molecules*; Wiley: New York, 1970; pp 301-71.
(19) Martinho, J. M. G.; Winnik, M. A. *J. Phys. Chem.* **1987**, *91*, 3640-4.
(20) (a) Hauser, M. *Acta Phys. Chem. Szeged* **1984**, *30*, 7-27. (b) Vogelsang, J.; Hauser, M. *J. Phys. Chem.* **1990**, *94*, 7488-94. (c) Vogelsang, J.; Hauser, M. *Ber. Bunsen. Phys. Chem.* **1990**, *94*, 1326-31.
(21) (a) Martinho, J. M. G.; Campos, V. M.; Tencer, M.; Winnik, M. A. *Macromolecules* **1987**, *20*, 1582-7. (b) Martinho, J. M. G.; Sienicki, K.; Blue, D.; Winnik, M. A. *Macromolecules* **1988**, *110*, 7773-7. (c) Martinho, J. M. G.; Tencer, M.; Campos, M.; Winnik, M. A. *Macromolecules* **1989**, *22*, 322-7. (d) Stukelj, M.; Martinho, J. M. G.; Winnik, M. A.; Quirk, R. P. *Macromolecules* **1991**, *24*, 2488-92.

Product Distributions of the C_2H_2 + O and HCCO + H Reactions. Rate Constant of $CH_2(\tilde{X}\,^3B_1)$ + H

Werner Boullart and Jozef Peeters*

Department of Chemistry, K.U. Leuven, Celestijnenlaan 200F, B-3001 Leuven, Belgium
(Received: May 7, 1992; In Final Form: August 17, 1992)

The branching ratios of the two dominant methylene sources in C_2H_2/O/H systems C_2H_2 + O → $CH_2(^3B_1)$ + CO (r2a) or HCCO + H (r2b) and HCCO + H → $CH_2(^1A_1)$ + CO (r3a) or $CH_2(^3B_1)$ + CO (r3b) have been determined, at 285 K, using discharge-flow/molecular beam mass spectrometry techniques (D-F/MBMS). The ratios were derived from the observed decreases of MBMS CH_2 signals upon substituting 25% of the helium bath gas by 0.5 Torr of methane, which selectively scavenges $CH_2(^1A_1)$; in the absence of CH_4 the singlet CH_2 is mainly collisionally converted to $CH_2(^3B_1)$. In this way, the ratios of the total formation rates of singlet and triplet CH_2 are obtained. As the rate of reaction r3 is linked to the rate of reaction r2b by the known fraction of HCCO reacting with H, in competition with O, both the ratios k_{2a}/k_{2b} and k_{3a}/k_{3b} can be extracted from the data. Thus, including also probably systematic errors, the HCCO yield of C_2H_2 + O is found to be $k_{2b}/k_2 = 85^{+4}_{-9}\%$ and the $CH_2(^1A_1)$ yield of HCCO + H, $k_{3a}/k_3 = 92 \pm 15\%$ (95% confidence intervals). In addition, the rate constant of $CH_2(^3B_1)$ + H → $CH(^2\Pi)$ + H_2 (r1) was derived relative to the known $k(^3CH_2+O)$ from CH_2 signals at different [H]/[O] ratios: $k_1 = (1.6 \pm 0.6) \times 10^{14}$ cm^3 mol^{-1} s^{-1}.

Introduction

The $CH_2(\tilde{X}\,^3B_1)$ and $CH_2(\tilde{a}\,^1A_1)$ radicals are likely precursors of higher unsaturated hydrocarbons and of aromatics in fossil-fuel combustion processes.

The role of $CH_2(^3B_1)$ is indirect: its reaction with H atoms is considered as the primary source of $CH(^2\Pi)$ radicals[1-3]

$$CH_2(^3B_1) + H \rightarrow CH(^2\Pi) + H_2 \qquad (r1)$$

which by their subsequent fast insertion or cycloaddition (in)to C_2H_2[4] will lead to unsatuated C_3 radicals. Direct k_1 determinations[3] have shown reaction r1 to be very fast at room temperature.

The importance of the $CH_2(^1A_1)$ radical—observed spectroscopically in C_2H_2/O/H systems at room temperature by Peeters et al.[5]—is of a kindred nature. Due to its high reactivity toward closed-shell molecules such as ethyne[6,7] and other hydrocarbons,[7,8]

0022-3654/92/2096-9810$03.00/0